Electronic Supplementary Information (ESI)

Very close I···As and I···Sb interactions in trimethylpnictogen-pentafluoroiodobenzene cocrystals

Maciej Bujak,*[a,b] Hans-Georg Stammler,[b] Yury V. Vishnevskiy,[b] and Norbert W. Mitzel*[b]

[a]*Faculty of Chemistry, University of Opole, Oleska 48, 45-052 Opole, Poland. E-mail: mbujak@uni.opole.pl*
[b]*Lehrstuhl für Anorganische Chemie und Strukturchemie, Fakultät für Chemie, Universität Bielefeld, Universitätsstr. 25, 33615 Bielefeld, Germany. E-mail: mitzel@uni-bielefeld.de*

Table of Contents

Table S1. Crystal data and structure determination summary for $(CH_3)_3As{\cdot}C_6F_5I$, **1** at 220, 180, 150 and 100 K.

formula	$C_9H_9AsF_5I$	$C_9H_9AsF_5I$	$C_9H_9AsF_5I$	$C_9H_9AsF_5I$
M_r	413.98	413.98	413.98	413.98
crystal size, mm	0.3 × 0.3 × 0.2	0.3 × 0.3 × 0.2	0.3 × 0.3 × 0.2	0.3 × 0.3 × 0.2
crystal system	monoclinic	monoclinic	monoclinic	monoclinic
space group, *Z, Z'*	*C2/c*, 8, 1	*C2/c*, 8, 1	*C2/c*, 8, 1	*C2/c*, 8, 1
temperature, K	220.0(1)	180.0(1)	150.0(1)	100.0(1)
a, Å	11.5901(3)	11.5215(3)	11.4664(3)	11.3040(2)
b, Å	11.6731(3)	11.6259(3)	11.5939(2)	11.5876(2)
c, Å	20.0896(5)	20.0623(5)	20.0447(4)	20.0586(4)
β, °	102.821(3)	102.807(3)	102.752(2)	102.512(2)
V, Å^3	2650.21(12)	2620.45(12)	2599.02(10)	2565.00(8)
ρ, g/cm^3	2.075	2.099	2.116	2.144
μ, mm^{-1}	4.925	4.981	5.022	5.089
θ range, °	2.08 - 26.00	2.08 - 26.00	2.08 - 26.00	2.08 - 26.00
index ranges	$-14 \le h \le 14$	$-14 \le h \le 14$	$-14 \le h \le 14$	$-13 \le h \le 13$
	$-14 \le k \le 14$	$-14 \le k \le 14$	$-14 \le k \le 14$	$-14 \le k \le 14$
	$-24 \le l \le 24$	$-24 \le l \le 24$	$-24 \le l \le 24$	$-24 \le l \le 24$
reflns collected	18349	18126	18082	17720
R_{int}	0.0399	0.0382	0.0280	0.0261
data [$I > 2\sigma(I)$]	2260	2345	2384	2386
data/parameters	2603/149	2574/149	2551/149	2510/148
GOF on F^2	1.041	1.041	1.092	1.142
R_1 [$I > 2\sigma(I)$]	0.0278	0.0245	0.0202	0.0183
R_1 (all data)	0.0333	0.0275	0.0224	0.0200
wR_2 (all data)	0.0730	0.0628	0.0498	0.0425
lrgst diff peak, *e*/Å^3	0.560	0.607	0.582	0.606
lrgst diff hole, *e*/Å^3	–0.406	–0.561	–0.530	–0.441
CCDC number	2057069	2057070	2057071	2057072

Table S2. Crystal data and structure determination summary for $(CH_3)_3Sb{\cdot}C_6F_5I$, **2** at 210, 180, 150 and 100 K.

formula	$C_9H_9F_5ISb$	$C_9H_9F_5ISb$	$C_9H_9F_5ISb$	$C_9H_9F_5ISb$
M_r	460.82	460.82	460.82	460.82
crystal size, mm	0.1 × 0.1 × 0.1	0.1 × 0.1 × 0.1	0.1 × 0.1 × 0.1	0.1 × 0.1 × 0.1
crystal system	monoclinic	monoclinic	monoclinic	monoclinic
space group, *Z, Z'*	*I2/a*, 8, 1	*I2/a*, 8, 1	*I2/a*, 8, 1	*I2/a*, 8, 1
temperature, K	210.0(1)	180.0(1)	150.0(1)	100.0(1)
a, Å	20.2334(16)	20.1543(14)	20.0697(14)	19.9342(16)
b, Å	6.0804(4)	6.0578(3)	6.0327(3)	5.9935(3)
c, Å	23.4856(16)	23.5026(14)	23.5298(14)	23.6586(14)
β, °	107.930(8)	108.230(7)	108.600(7)	109.451(7)
V, Å^3	2749.0(4)	2725.4(3)	2700.1(3)	2665.3(3)
ρ, g/cm^3	2.227	2.246	2.267	2.297
μ, mm^{-1}	4.283	4.320	4.360	4.417
θ range, °	1.82 - 26.00	2.13 - 26.00	2.14 - 26.00	2.17 - 26.00
index ranges	$-24 \le h \le 24$	$-24 \le h \le 24$	$-24 \le h \le 24$	$-24 \le h \le 24$
	$-7 \le k \le 7$	$-7 \le k \le 7$	$-7 \le k \le 7$	$-7 \le k \le 7$
	$-28 \le l \le 28$	$-28 \le l \le 28$	$-29 \le l \le 29$	$-29 \le l \le 29$
reflns collected	18500	18159	17700	16495
R_{int}	0.0544	0.0509	0.0493	0.0583
data [$I > 2\sigma(I)$]	2363	2423	2408	2394
data/parameters	2714/149	2686/148	2656/148	2627/148
GOF on F^2	1.051	1.090	1.097	1.072
R_1 [$I > 2\sigma(I)$]	0.0273	0.0270	0.0252	0.0275
R_1 (all data)	0.0329	0.0314	0.0295	0.0312
wR_2 (all data)	0.0663	0.0624	0.0565	0.0629
lrgst diff peak, *e*/Å^3	0.920	0.890	0.651	0.943
lrgst diff hole, *e*/Å^3	–0.795	–0.704	–0.643	–0.622
CCDC number	2057073	2057074	2057075	2057076

Table S3. Crystal data and structure determination summary for $(CH_3)_3As$, **3** at 150, 125 and 100 K.

formula	C_3H_9As	C_3H_9As	C_3H_9As
M_r	120.02	120.02	120.02
crystal size, mm	0.2 × 0.2 × 0.1	0.2 × 0.2 × 0.1	0.2 × 0.2 × 0.1
crystal system	orthorhombic	orthorhombic	orthorhombic
space group, *Z*, *Z'*	$Cmc2_1$, 4, 0.5	$Cmc2_1$, 4, 0.5	$Cmc2_1$, 4, 0.5
temperature, K	150.0(1)	125.0(1)	100.0(1)
a, Å	9.3417(7)	9.3043(5)	9.2883(2)
b, Å	10.9779(7)	10.9531(6)	10.9515(3)
c, Å	5.2141(3)	5.1983(2)	5.18635(13)
V, Å^3	534.72(6)	529.76(5)	527.56(2)
ρ, g/cm^3	1.491	1.505	1.511
μ, mm^{-1}	6.179	6.237	6.263
θ range, °	2.86 - 25.89	2.87 - 26.00	2.88 - 25.97
index ranges	$-11 \le h \le 11$	$-11 \le h \le 11$	$-11 \le h \le 11$
	$-13 \le k \le 13$	$-13 \le k \le 13$	$-13 \le k \le 13$
	$-6 \le l \le 6$	$-6 \le l \le 6$	$-6 \le l \le 6$
reflns collected	4078	4052	12544
R_{int}	0.0303	0.0291	0.0416
data [$I > 2\sigma(I)$]	546	550	549
data/parameters	554/29	554/29	551/29
GOF on F^2	1.101	1.119	1.106
R_1 [$I > 2\sigma(I)$]	0.0481	0.0478	0.0191
R_1 (all data)	0.0486	0.0478	0.0192
wR_2 (all data)	0.1227	0.1210	0.0498
lrgst diff peak, *e*/Å^3	0.277	0.326	0.287
lrgst diff hole, *e*/Å^3	–0.520	–0.495	–0.275
CCDC number	2057063	2057064	2057065

Table S4. Crystal data and structure determination summary for $(CH_3)_3Sb$, **4** at 170, 150 and 100 K.

formula	C_3H_9Sb	C_3H_9Sb	C_3H_9Sb
M_r	166.86	166.86	166.86
crystal size, mm	0.3 × 0.3 × 0.3	0.3 × 0.3 × 0.3	0.3 × 0.3 × 0.3
crystal system	monoclinic	monoclinic	monoclinic
space group, *Z*, *Z'*	$P2_1/n$, 4, 1	$P2_1/n$, 4, 1	$P2_1/n$, 4, 1
temperature, K	170.0(1)	150.0(1)	100.0(1)
a, Å	6.12026(13)	6.09729(11)	6.04482(9)
b, Å	11.2342(2)	11.20824(19)	11.14435(16)
c, Å	8.55360(16)	8.52671(15)	8.48341(13)
β, °	96.8027(19)	96.7940(17)	96.8289(14)
V, Å^3	583.97(2)	578.623(18)	567.436(15)
ρ, g/cm^3	1.898	1.916	1.953
μ, mm^{-1}	4.562	4.604	4.695
θ range, °	3.81 - 26.00	3.02 - 26.00	4.33 - 26.00
index ranges	$-7 \le h \le 7$	$-7 \le h \le 7$	$-7 \le h \le 7$
	$-13 \le k \le 13$	$-13 \le k \le 13$	$-13 \le k \le 13$
	$-10 \le l \le 10$	$-10 \le l \le 10$	$-10 \le l \le 10$
reflns collected	7680	7596	7411
R_{int}	0.0250	0.0243	0.0240
data [$I > 2\sigma(I)$]	1097	1090	1089
data/parameters	1139/41	1128/41	1103/41
GOF on F^2	1.103	1.085	1.171
R_1 [$I > 2\sigma(I)$]	0.0146	0.0134	0.0123
R_1 (all data)	0.0159	0.0145	0.0126
wR_2 (all data)	0.0348	0.0294	0.0271
lrgst diff peak, *e*/Å^3	0.354	0.447	0.408
lrgst diff hole, *e*/Å^3	–0.424	–0.280	–0.236
CCDC number	2057066	2057067	2057068

Table S5. Molecular dimensions (Å, º) for $(CH_3)_3As{\cdot}C_6F_5I$, **1** at 220, 180, 150 and 100 K.

Temperature, K	220	180	150	100
As1–C1	1.920(5)	1.933(5)	1.936(4)	1.942(3)
As1–C2	1.938(5)	1.936(4)	1.939(3)	1.944(3)
As1–C3	1.949(5)	1.945(4)	1.949(3)	1.950(3)
C1–As1–C2	97.7(3)	98.0(2)	98.05(18)	97.87(15)
C1–As1–C3	98.5(2)	98.6(2)	98.44(16)	98.61(14)
C2–As1–C3	98.8(2)	98.8(2)	98.77(16)	98.88(14)
I1–C4	2.096(4)	2.096(3)	2.100(3)	2.101(2)
F1–C5	1.335(5)	1.341(4)	1.340(4)	1.339(3)
F2–C6	1.341(6)	1.334(5)	1.339(4)	1.342(4)
F3–C7	1.352(6)	1.352(5)	1.347(4)	1.346(4)
F4–C8	1.342(6)	1.343(5)	1.339(4)	1.342(4)
F5–C9	1.333(5)	1.328(5)	1.334(4)	1.339(4)
C4–C5	1.380(6)	1.381(5)	1.375(4)	1.379(4)
C4–C9	1.378(5)	1.380(5)	1.380(4)	1.378(4)
C5–C6	1.367(6)	1.371(5)	1.379(4)	1.382(4)
C6–C7	1.372(8)	1.382(7)	1.378(6)	1.380(6)
C7–C8	1.355(8)	1.366(8)	1.363(6)	1.364(6)
C8–C9	1.372(6)	1.375(6)	1.375(5)	1.379(4)
C5–C4–I1	121.0(3)	121.3(3)	121.2(2)	120.9(2)
C9–C4–I1	120.8(3)	120.5(3)	120.6(2)	121.0(2)
F1–C5–C4	120.3(4)	120.1(3)	120.5(3)	120.8(2)
F1–C5–C6	118.7(5)	118.1(4)	118.1(3)	118.0(3)
F2–C6–C5	119.8(6)	120.7(5)	120.2(4)	120.3(4)
F2–C6–C7	120.8(5)	120.8(4)	120.9(3)	120.5(3)
F3–C7–C6	119.3(6)	118.7(6)	118.5(4)	119.1(4)
F3–C7–C8	120.1(7)	120.3(6)	120.6(4)	120.2(4)
F4–C8–C7	120.3(5)	120.1(4)	120.2(4)	120.1(3)
F4–C8–C9	119.8(6)	120.3(5)	120.4(4)	120.5(4)
F5–C9–C4	120.7(4)	121.1(3)	121.0(3)	120.8(3)
F5–C9–C8	118.4(5)	117.9(4)	117.8(3)	117.7(3)
C4–C5–C6	121.0(5)	121.8(4)	121.4(3)	121.2(3)
C4–C9–C8	120.9(5)	121.0(4)	121.2(3)	121.5(3)
C5–C4–C9	118.2(4)	118.2(3)	118.2(3)	118.1(3)
C5–C6–C7	119.5(5)	118.5(4)	118.8(3)	119.2(3)
C6–C7–C8	120.6(5)	121.0(4)	120.9(3)	120.6(3)
C7–C8–C9	119.8(5)	119.5(4)	119.4(4)	119.4(3)

Table S6. Molecular dimensions (Å, º) for $(CH_3)_3Sb{\cdot}C_6F_5I$, **2** at 210, 180, 150 and 100 K.

Temperature, K	210	180	150	100
Sb1–C1	2.127(6)	2.124(6)	2.128(5)	2.130(5)
Sb1–C2	2.132(5)	2.131(5)	2.140(4)	2.145(5)
Sb1–C3	2.099(6)	2.109(5)	2.115(5)	2.126(5)
C1–Sb1–C2	95.9(2)	95.8(2)	95.9(2)	95.7(2)
C1–Sb1–C3	94.0(3)	94.6(3)	94.9(3)	95.2(2)
C2–Sb1–C3	96.4(3)	96.3(2)	96.1(2)	95.7(2)
I1–C4	2.096(4)	2.097(3)	2.097(3)	2.097(4)
F1–C5	1.343(5)	1.346(4)	1.348(4)	1.350(5)
F2–C6	1.341(5)	1.342(4)	1.337(4)	1.345(4)
F3–C7	1.339(5)	1.337(4)	1.335(4)	1.334(5)
F4–C8	1.339(5)	1.338(4)	1.341(4)	1.341(5)
F5–C9	1.335(4)	1.339(4)	1.337(4)	1.339(4)
C4–C5	1.377(5)	1.382(5)	1.379(5)	1.382(5)
C4–C9	1.372(5)	1.377(5)	1.377(5)	1.382(6)
C5–C6	1.369(6)	1.365(5)	1.367(5)	1.367(6)
C6–C7	1.370(7)	1.373(6)	1.375(6)	1.377(6)
C7–C8	1.377(6)	1.378(6)	1.381(5)	1.383(6)
C8–C9	1.371(5)	1.371(5)	1.371(5)	1.371(6)
C5–C4–I1	120.9(3)	121.1(3)	121.2(3)	121.2(3)
C9–C4–I1	121.3(3)	121.4(3)	121.2(2)	121.2(3)
F1–C5–C4	120.3(3)	119.8(3)	119.9(3)	119.8(4)
F1–C5–C6	117.8(3)	118.3(3)	118.1(3)	118.4(3)
F2–C6–C5	120.5(4)	120.3(4)	120.3(4)	120.2(4)
F2–C6–C7	120.4(4)	120.3(4)	120.3(3)	120.0(4)
F3–C7–C6	120.3(4)	120.3(4)	120.4(3)	120.6(4)
F3–C7–C8	119.3(4)	119.4(4)	119.8(3)	119.7(4)
F4–C8–C7	119.6(4)	119.5(4)	119.2(3)	119.0(4)
F4–C8–C9	121.2(4)	121.2(4)	121.2(3)	121.4(4)
F5–C9–C4	120.5(3)	120.2(3)	120.4(3)	120.2(3)
F5–C9–C8	117.8(3)	118.1(3)	118.0(3)	118.2(4)
C4–C5–C6	121.9(4)	121.9(4)	122.0(3)	121.8(4)
C4–C9–C8	121.7(4)	121.7(3)	121.6(3)	121.7(4)
C5–C4–C9	117.7(3)	117.5(3)	117.6(3)	117.5(4)
C5–C6–C7	119.1(4)	119.4(3)	119.4(3)	119.8(4)
C6–C7–C8	120.4(4)	120.2(3)	119.8(3)	119.7(4)
C7–C8–C9	119.2(4)	119.3(3)	119.6(3)	119.6(4)

Table S7. Molecular dimensions (Å, º) for $(CH_3)_3As$, **3** at 150, 125 and 100 K (single crystal X-ray diffraction), compared to those determined by gas electron diffraction.[1]

Method	single crystal X-ray diffraction			gas electron diffraction
Temperature, K	150	125	100	
As1–C1/C1^{I}	1.961(9)	1.958(9)	1.963(4)	1.968(3)
As1–C2	1.960(3)	1.958(3)	1.963(3)	
C1–As1–CI^{I}	96.2(6)	96.0(5)	96.3(2)	96.1(5)
C1/C1^{I}–As1–C2	96.6(3)	97.0(3)	96.85(12)	
Symmetry code: (I) 1 – *x*, *y*, *z*.				

Table S8. Molecular dimensions (Å, º) for $(CH_3)_3Sb$, **4** at 170, 150 and 100 K (single crystal X-ray diffraction), compared to those determined by gas electron diffraction.[1]

Method	single crystal X-ray diffraction			gas electron diffraction
Temperature, K	170	150	100	
Sb1–C1	2.141(2)	2.143(2)	2.1468(19)	
Sb1–C2	2.144(3)	2.146(2)	2.151(2)	2.163(3)
Sb1–C3	2.143(2)	2.148(2)	2.1538(18)	
C1–Sb1–C2	94.14(10)	94.08(9)	94.09(8)	
C1–Sb1–C3	95.13(11)	95.15(10)	94.99(8)	94.1(5)
C2–Sb1–C3	94.97(11)	94.89(10)	94.84(8)	

Table S9. Dimensions (Å, º) of the intermolecular contacts for $(CH_3)_3As{\cdot}C_6F_5I$, **1** at 220, 180 and 150 K, compared to those commensurate with the sums of the van der Waals radii of respective atoms at 100 K.[2]

Temperature, K	220	180	150	100
I1···As1	3.3671(5)	3.3469(4)	3.3314(3)	3.3044(3)
C4–I1···As1	171.50(9)	171.50(8)	171.57(7)	171.60(6)
I1···As1–C1	119.9(2)	119.57(16)	119.32(13)	118.02(11)
I1···As1–C2	106.11(15)	105.63(13)	105.37(10)	105.24(9)
I1···As1–C3	129.71(15)	130.16(13)	130.70(10)	131.90(9)
F4···F4^{I}	2.910(6)	2.892(6)	2.885(4)	2.886(4)
C8–F4···F4^{I}	85.5(3)	84.9(2)	84.50(18)	83.37(17)
F4···F4^{I}–C8^{I}	85.5(3)	84.9(2)	84.50(18)	83.37(17)
F2···C6^{II}	3.037(5)	3.012(4)	3.001(4)	2.984(3)
C6–F2···C6^{II}	106.0(3)	105.6(2)	105.18(17)	104.76(16)
F2···C6^{II}–C5^{II}	109.8(3)	110.0(2)	110.22(19)	111.88(18)
F2···C6^{II}–C7^{II}	85.9(3)	85.0(3)	84.4(2)	82.2(2)
C6···F2^{II}	3.037(5)	3.012(4)	3.001(4)	2.984(3)
C5–C6···F2^{II}	109.8(3)	110.0(2)	110.22(19)	111.88(18)
C7–C6···F2^{II}	85.9(3)	85.0(3)	84.4(2)	82.2(2)
C6···F2^{II}–C6^{II}	106.0(3)	105.6(2)	105.18(17)	104.76(16)
F2···C7^{II}	3.243(7)	3.202(6)	3.178(4)	3.114(4)
C6–F2···C7^{II}	118.3(3)	118.3(3)	118.03(19)	117.98(18)
F2···C7^{II}–C6^{II}	69.1(3)	69.6(3)	70.0(2)	71.74(19)
F2···C7^{II}–C8^{II}	117.5(3)	117.3(3)	117.2(2)	116.9(2)
C7···F2^{II}	3.243(7)	3.202(6)	3.178(4)	3.114(4)
C6–C7···F2^{II}	69.1(3)	69.6(3)	70.0(2)	71.74(19)
C8–C7···F2^{II}	117.5(3)	117.3(3)	117.2(2)	116.9(2)
C7···F2^{II}–C6^{II}	118.3(3)	118.3(3)	118.0(2)	117.98(18)
F4···C8^{I}	3.108(6)	3.079(5)	3.062(4)	3.039(4)
C8–F4···C8^{I}	111.0(3)	110.7(2)	110.3(2)	109.38(17)
F4···C8^{I}–C7^{I}	96.4(3)	96.2(3)	96.5 (2)	98.0(2)
F4···C8^{I}–C9^{I}	103.8(3)	103.6(3)	103.1(2)	100.9(2)
C8···F4^{I}	3.108(6)	3.079(5)	3.062(4)	3.039(4)
C7–C8···F4^{I}	96.4(3)	96.2(3)	96.5(2)	98.0(2)
C9–C8···F4^{I}	103.8(3)	103.6(3)	103.1(2)	100.9(2)
C8···F4^{I}–C8^{I}	111.0(3)	110.7(2)	110.3(2)	109.38(17)
F4···H21^{III}	2.71	2.69	2.67	2.66
C8–F4···H21^{III}	139	139	139	141
F4···H21^{III}–C2^{III}	133	131	130	129
H21···F4^{III}	2.71	2.69	2.67	2.66
C2–H21···F4^{III}	133	131	130	129
H21···F4^{III}–C8^{III}	139	139	139	141
Symmetry codes: (I) –1/2 – *x*, 1/2 – *y*, 1 – *z*; (II) –*x*, –*y*, 1 – *z*; (III) –*x*, 1 – *y*, 1 – *z*.				

Table S10. Dimensions (Å, º) of the intermolecular contacts for $(CH_3)_3Sb{\cdot}C_6F_5I$, **2** at 210, 180 and 150 K, compared to those commensurate with the sums of the van der Waals radii of respective atoms at 100 K.[2]

Temperature, K	210	180	150	100
I1···Sb1	3.5457(4)	3.5297(4)	3.5150(4)	3.4951(4)
C4–I1···Sb1	171.94(10)	172.13(10)	172.23(10)	172.22(11)
I1···Sb1–C1	135.4(3)	135.4(2)	135.28(19)	135.34(18)
I1···Sb1–C2	113.52(15)	113.65(14)	113.89(12)	114.43(13)
I1···Sb1–C3	113.9(2)	113.48(17)	113.08(15)	112.66(15)
F1···F2^{I}	2.876(4)	2.854(3)	2.835(3)	2.802(3)
C5–F1···F2^{I}	140.3(2)	139.9(2)	140.0(2)	139.8(2)
F1···F2^{I}–C6^{I}	126.0(3)	126.3(2)	127.1(2)	128.7(2)
F2···F1^{II}	2.876(4)	2.854(3)	2.835(3)	2.802(3)
C6–F2···F1^{II}	126.0(3)	126.3(2)	127.1(2)	128.7(2)
F2···F1^{II}–C5^{II}	140.3(2)	139.9(2)	140.0(2)	139.8(2)
F4···H21^{III}	2.59	2.56	2.58	2.58
C8–F4···H21^{III}	138	139	138	138
F4···H21^{III}–C2^{III}	138	139	136	134
H21···F4^{III}	2.59	2.56	2.58	2.58
C2–H21···F4^{III}	138	139	136	134
H21···F4^{III}–C8^{III}	138	139	138	138
Symmetry codes: (I) 1 – *x*, –1/2 + *y*, 3/2 – *z*; (II) 1 – *x*, 1/2 + *y*, 3/2 – *z*; (III) 1 – *x*, 2 – *y*, 1 – *z*.				

Table S11. Dimensions (Å, º) of the intermolecular Sb···Sb contacts for $(CH_3)_3Sb$, **4** at 170 and 150 K, compared to those commensurate with the sum of the van der Waals radii of Sb atoms at 100 K.[2]

Temperature, K	170	150	100
Sb1···Sb1^{I}	3.8706(3)	3.8591(3)	3.8374(2)
C1–Sb1···Sb1^{I}	85.90(7)	85.90(7)	85.92(6)
C2–Sb1···Sb1^{I}	91.92(7)	92.19(7)	92.83(6)
C3–Sb1···Sb1^{I}	172.94(8)	172.75(7)	172.20(6)
Sb1···Sb1^{I}–C1^{I}	85.90(7)	85.90(7)	85.92(6)
Sb1···Sb1^{I}–C2^{I}	91.92(7)	92.19(7)	92.83(6)
Sb1···Sb1^{I}–C3^{I}	172.94(8)	172.75(7)	172.20(6)
Symmetry code: (I) 1–*x*, 1–*y*, 1–*z*.			

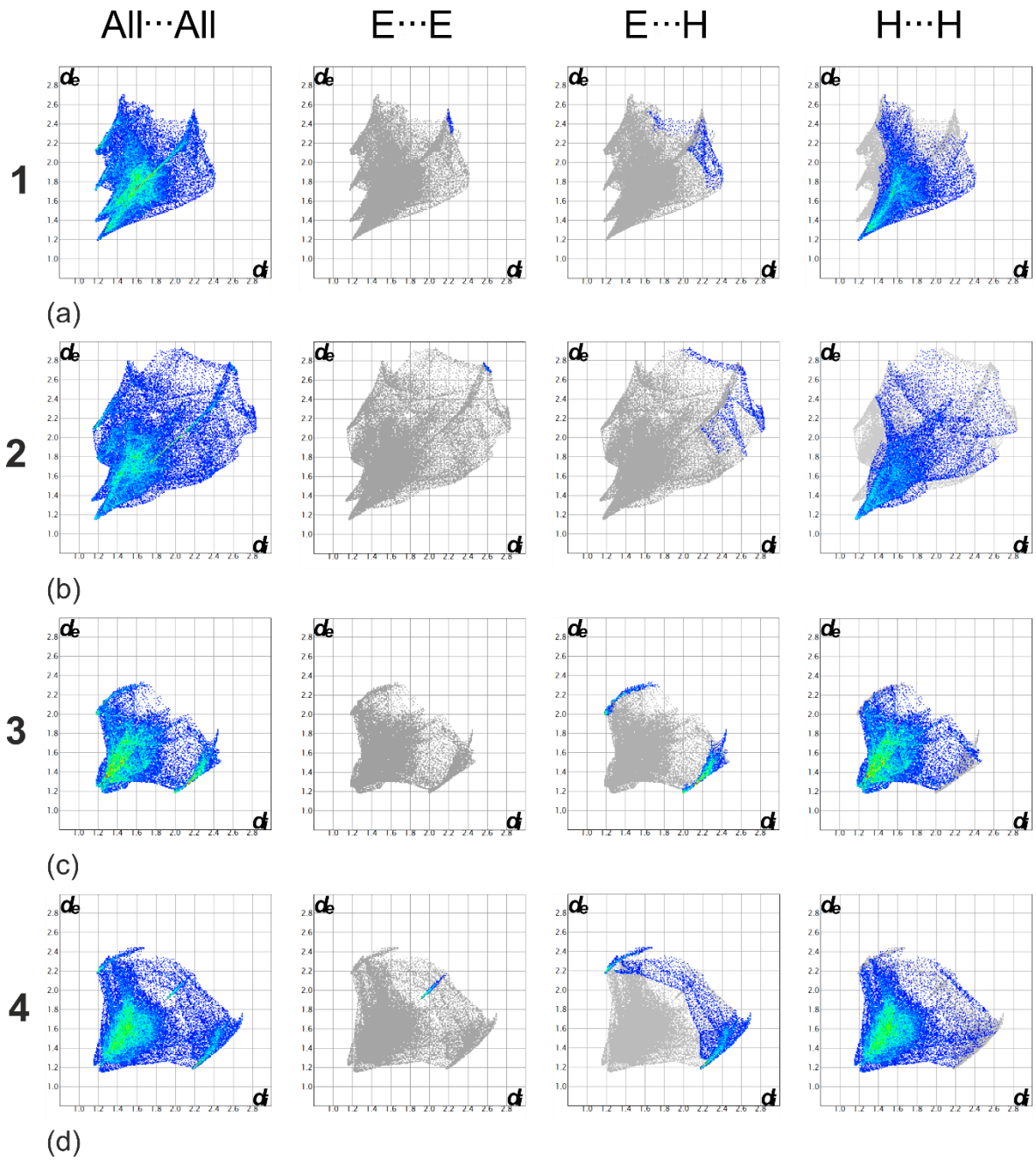

Figure S1. Fingerprint plots for $(CH_3)_3E$ molecules, at 100 K, in: **1** (a), **2** (b), **3** (c) and **4** (d) along with the highlighted E···E, E···H and H···H contacts (E = As for **1** and **3**, and E = Sb for **2** and **4**).

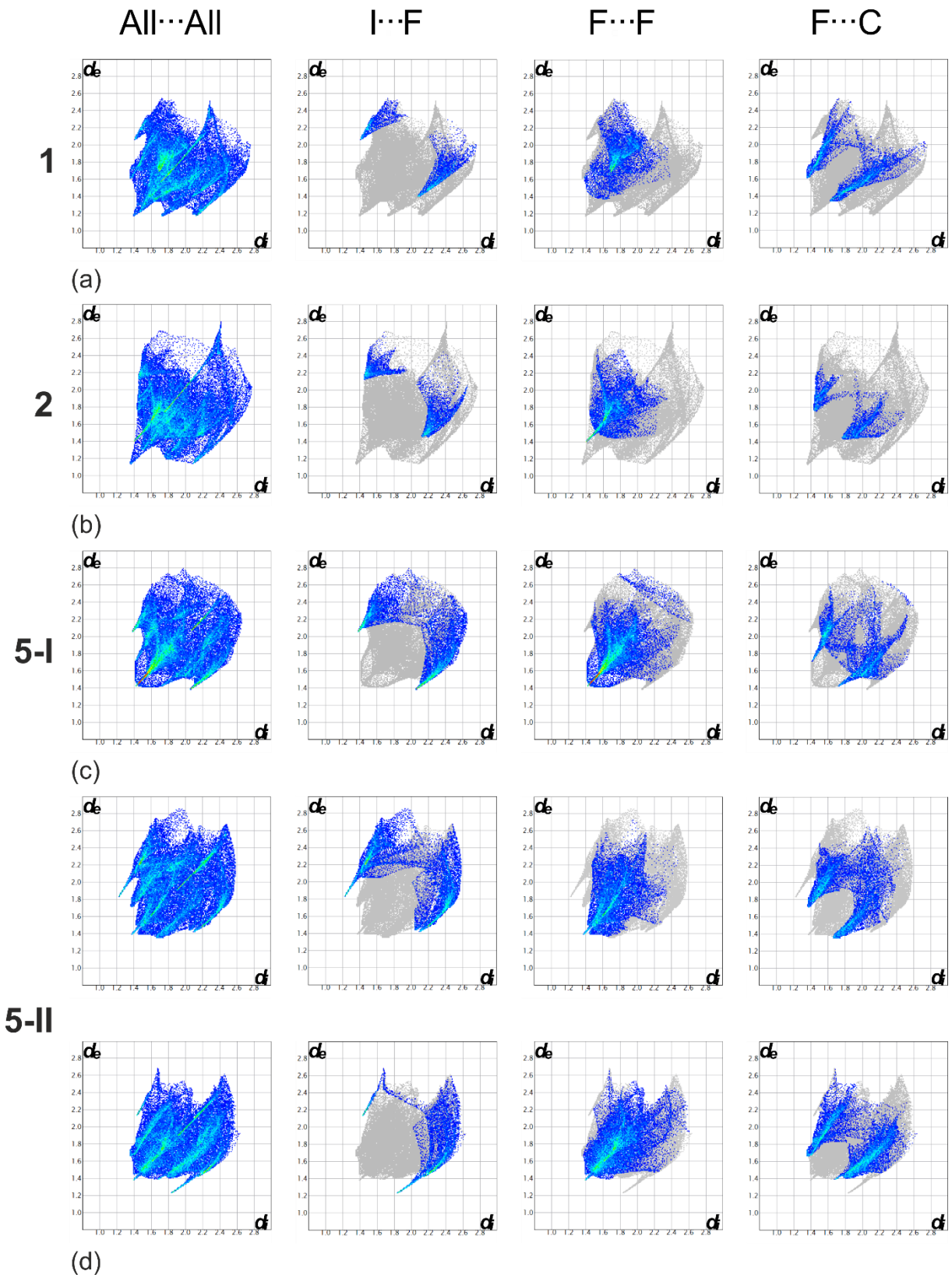

Figure S2. Fingerprint plots for C_6F_5I molecules in: **1** (a), **2** (b), **5-I**[3a] (c) and **5-II**[3b] (d, note two symmetry independent molecules, upper C11-C16 and lower C21-C26) along with the highlighted I···F, F···F and F···C contacts. The structures of **1**, **2** and **5-II** were determined at 100 K, whereas **5-I** at 150 K.

Quantum-chemical calculations

Geometry optimizations and the calculations on **1**–**5** were performed using the Gaussian 09 program package[4] along with the GaussView 5.0 software as a graphical interface.[5] The DFT calculations were carried out at the B3LYP/3–21G* level of theory,[6] in vacuum, for the geometries obtained from the X-ray diffraction results as an input.[3a] The molecular isodensity surfaces for **1**-**5** mapped with their electrostatic potential along with the calculated partial atomic charges (NBO), for selected atoms, are depicted in Figure S3. To further understand the nature of interactions in **1** and **2** the described below studies were carried out.

In the first stage the calibration of theoretical approximations was performed - two small model systems, $H_3As\cdots ICH_3$ and $H_3Sb\cdots ICH_3$, were investigated. Their geometries were fully optimized using the CCSD(T)[7] level of theory with basis sets from the cc-pwCVnZ (n = 2, 3, 4) family,[8] small-core pseudopotentials for As, Sb and I atoms within respective cc-pwCVnZ-PP sets,[9] and in all-electron variant for the other atoms.[10] From the results extrapolations of r(I···E) distances (E = As or Sb) to the complete basis set limit were done. Also, the stabilization energies were calculated. The energies for the complete basis set (CBS) limit were obtained by fitting to the exponential function in the same way as for geometrical parameters. In addition, several lower-level calculations for the same two molecules were carried out. The geometry optimizations were done with DFT using PBE0-D3BJ/def2-QZVPP[11,12] and frozen-core spin-component-scaled MP2/def2-TZVPP[13,14] levels of theory as implemented in Gaussian 16 program package.[15] Stabilization energies were also computed for the aforementioned DFT and MP2 geometries using single-point frozen-core DLPNO-CCSD(T)/def2-QZVPP[16] calculations (with the TightPNO setting) in Orca 4.2.1.[17] The results of these calculations are summarized in Tables S12 and S13. It is clear, from these data, that the stated above DFT approximation gave the closest r_e(I···E) distance to the reference values from the coupled cluster estimations for the complete basis set limit. Using the same reference for the stabilization energies the best affordable level of theory was DLPNO-CCSD(T)/def2-QZVPP. The dependence on used geometrical structures in these single-point calculations was found to be minimal. Thus, based on the calibration procedure, the DLPNO-CCSD(T)/def2-QZVPP//PBE0-D3BJ/def2-QZVPP level of theory was determined as the most accurate and has been used in all the subsequent calculations. The computed equilibrium distances I···E in $(CH_3)_3As\cdots IC_6F_5$ and $(CH_3)_3Sb\cdots IC_6F_5$ are 3.249 and 3.469 Å, respectively. The binding energies for these two systems are −4.96 and −4.12 kcal mol^{-1}, respectively (note, the estimated accuracy is about 0.1 Å and 0.1 kcal mol^{-1} with respect to the canonical CCSD(T)/CBS approximation).

To understand the nature of interactions between $(CH_3)_3E$ (E = As or Sb) and C_6F_5I components in $(CH_3)_3E\cdots IC_6F_5$ systems the local energy decomposition (LED) analysis[18] was applied. For comparison the same analysis was also performed for the two calibration molecules and for simple systems $H_3N\cdots ClF$, $HF\cdots HF$ and $CH_4\cdots CH_4$. The results are collected in Table 1 of the paper. Figure S4 shows the dispersion interaction densities (DID)[19] in $(CH_3)_3E\cdots IC_6F_5$ (E = As or Sb). DID is the electron density associated with the dispersion component of the interaction energy in LED analysis. This property is calculated in analogy to the earlier

investigations[20] based on MP2 method. Note, here DID is related only to the intermolecular interaction and does not show intramolecular dispersion. Interestingly, in $(CH_3)_3E\cdots IC_6F_5$ systems DID is located not only on frontier atoms but also on E–C bonds (on As–C to a larger extent), whereas the atoms in the aromatic rings are not affected.

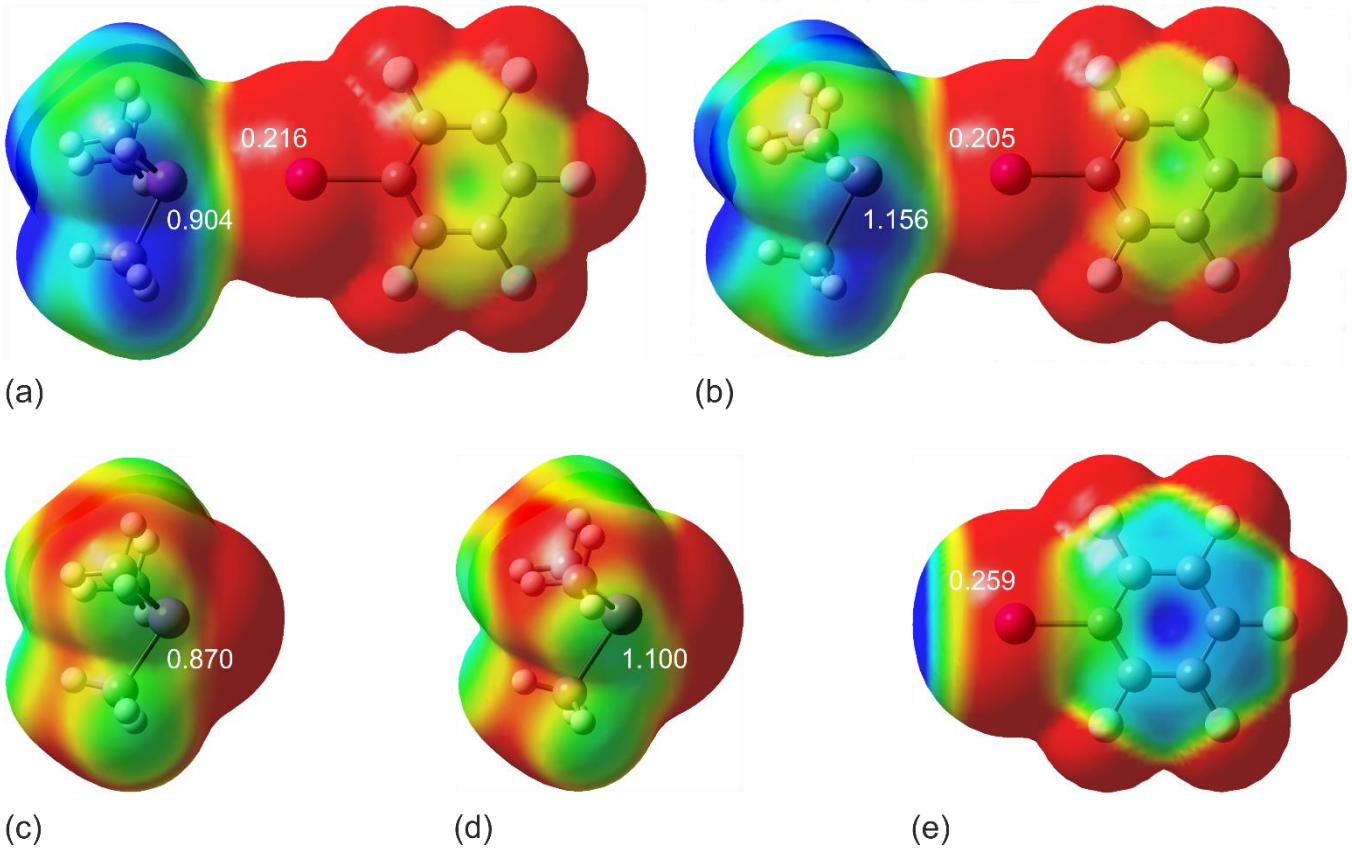

Figure S3. Molecular isodensity surfaces for **1** (a), **2** (b), **3** (c), **4** (d) and **5**[3a] (e) mapped with their electrostatic potential. The colours show positive from 0.02 a.u. (blue) to negative –0.002 a.u (red) and intermediate degrees (orange-green) of electrostatic potential. The calculated partial atomic charges (NBO), for the selected atoms, are also provided.

Table S12. Optimized equilibrium distances *r*(I···E) (Å) in $H_3E\cdots ICH_3$ at different levels of theory. E = As or Sb.

	PBE0-D3BJ/def2-QZVPP	fc-SCS-MP2/def2-TZVPP	ae-CCSD(T)/cc-pwCVDZ-PP	ae-CCSD(T)/cc-pwCVTZ-PP	ae-CCSD(T)/cc-pwCVQZ-PP	ae-CCSD(T)/CBS-PP
$H_3As\cdots ICH_3$	3.704	3.890	4.017	3.918	3.844	3.625
$H_3Sb\cdots ICH_3$	3.851	4.046	4.251	4.095	3.995	3.816

Table S13. Stabilization energies (kcal mol^{-1}) of $H_3E\cdots ICH_3$ calculated at different theoretical levels. E = As or Sb.

	PBE0-D3BJ/def2-QZVPP	fc-SCS-MP2/def2-TZVPP	DLPNO-CCSD(T)/def2-QZVPP//PBE0-D3BJ/def2-QZVPP	DLPNO-CCSD(T)/def2-QZVPP//fc-SCS-MP2/def2-TZVPP	ae-CCSD(T)/cc-pwCVDZ-PP	ae-CCSD(T)/cc-pwCVTZ-PP	ae-CCSD(T)/cc-pwCVQZ-PP	ae-CCSD(T)/CBS-PP
$H_3As\cdots ICH_3$	–1.96	–1.39	–1.52	–1.56	–1.00	–1.15	–1.36	–1.64
$H_3Sb\cdots ICH_3$	–2.03	–1.33	–1.57	–1.58	–0.89	–1.16	–1.43	–1.66

Table S14. Equilibrium Cartesian coordinates of atoms in $(CH_3)_3As\cdots IC_6F_5$ optimized at the PBE0-D3BJ/def2-QZVPP level.

As	3.70052	0.00055	–0.00007
C	4.63083	–1.21907	–1.20951
H	5.71122	–1.11835	–1.10389
H	4.33682	–2.24282	–0.98250
H	4.34322	–0.99532	–2.23580
C	4.64070	1.65318	–0.44781
H	4.35302	1.96948	–1.44942
H	4.35320	2.43173	0.25734
H	5.72024	1.50629	–0.40820
C	4.63283	–0.44273	1.65830
H	4.34607	0.26797	2.43208
H	4.33950	–1.44139	1.97874
H	5.71305	–0.40882	1.51496
I	0.45114	0.00218	–0.00019
C	–1.65381	0.00065	–0.00005
C	–2.36570	–1.18704	–0.00001
C	–2.36746	1.18728	–0.00001
C	–3.75030	–1.19959	0.00006
C	–3.75208	1.19776	0.00006
C	–4.44468	–0.00143	0.00009
F	–1.73805	2.35536	–0.00004
F	–4.41906	2.34237	0.00010
F	–5.76668	–0.00241	0.00016
F	–4.41558	–2.34518	0.00010
F	–1.73457	–2.35420	–0.00004

Table S15. Equilibrium Cartesian coordinates of atoms in $(CH_3)_3Sb\cdots IC_6F_5$ optimized at the PBE0-D3BJ/def2-QZVPP level.

Sb	3.50060	–0.00002	–0.00019
C	4.59897	–1.49162	–1.08413
H	5.66806	–1.32309	–0.95932
H	4.33934	–2.48041	–0.70931
H	4.34230	–1.43797	–2.14095
C	4.59793	1.68619	–0.74763
H	4.34107	1.85502	–1.79221
H	4.33779	2.57436	–0.17397
H	5.66714	1.49589	–0.66095
C	4.59504	–0.19416	1.83584
H	4.33540	0.62542	2.50406
H	4.33608	–1.13579	2.31739
H	5.66457	–0.17186	1.62955
I	0.03145	–0.00009	–0.00077
C	–2.06666	–0.00003	–0.00026
C	–2.77807	–1.18834	–0.00009
C	–2.77799	1.18833	–0.00009
C	–4.16268	–1.19887	0.00023
C	–4.16261	1.19895	0.00023
C	–4.85591	0.00006	0.00039
F	–2.14709	2.35462	–0.00022
F	–4.82834	2.34368	0.00039
F	–6.17741	0.00010	0.00069
F	–4.82849	–2.34356	0.00040
F	–2.14724	–2.35468	–0.00022

Table S16. Equilibrium Cartesian coordinates of atoms in $H_3As\cdots ICH_3$ optimized at the PBE0-D3BJ/def2-QZVPP level.

I	0.00000	0.00000	1.18047
C	0.00000	0.00000	3.31119
H	0.89376	–0.51601	3.64467
H	0.00000	1.03203	3.64467
H	–0.89376	–0.51601	3.64467
As	0.00000	0.00000	–2.52400
H	0.00000	1.26941	–3.35814
H	–1.09934	–0.63471	–3.35814
H	1.09934	–0.63471	–3.35814

Table S17. Equilibrium Cartesian coordinates of atoms in $H_3Sb\cdots ICH_3$ optimized at the PBE0-D3BJ/def2-QZVPP level.

I	0.00000	0.00000	1.64349
C	0.00000	0.00000	3.77489
H	0.00000	–1.03236	4.10712
H	0.89405	0.51618	4.10712
H	–0.89405	0.51618	4.10712
Sb	0.00000	0.00000	–2.20779
H	0.00000	1.41480	–3.15943
H	–1.22525	–0.70740	–3.15943
H	1.22525	–0.70740	–3.15943

Table S18. Equilibrium Cartesian coordinates of atoms in $H_3N\cdots ClF$ optimized at the PBE0-D3BJ/def2-QZVPP level.

N	0.00000	0.00000	–1.99989
H	0.00000	0.95271	–2.33536
H	–0.82507	–0.47636	–2.33536
H	0.82507	–0.47636	–2.33536
Cl	0.00000	0.00000	0.22025
F	0.00000	0.00000	1.91790

Table S19. Equilibrium Cartesian coordinates of atoms in $HF\cdots HF$ optimized at the PBE0-D3BJ/def2-QZVPP level.

F	0.03766	–1.29284	0.00000
H	–0.83023	–1.60049	0.00000
F	0.03766	1.41543	0.00000
H	0.15228	0.49717	0.00000

Table S20. Equilibrium Cartesian coordinates of atoms in $CH_4\cdots CH_4$ optimized at the PBE0-D3BJ/def2-QZVPP level.

C	0.00000	0.00000	1.85854
H	0.00000	1.02551	1.49424
H	–0.88812	–0.51275	1.49424
H	0.88812	–0.51275	1.49424
H	0.00000	0.00000	2.94686
C	0.00000	0.00000	–1.85854
H	0.00000	0.00000	–2.94686
H	–0.88812	0.51275	–1.49424
H	0.00000	–1.02551	–1.49424
H	0.88812	0.51275	–1.49424

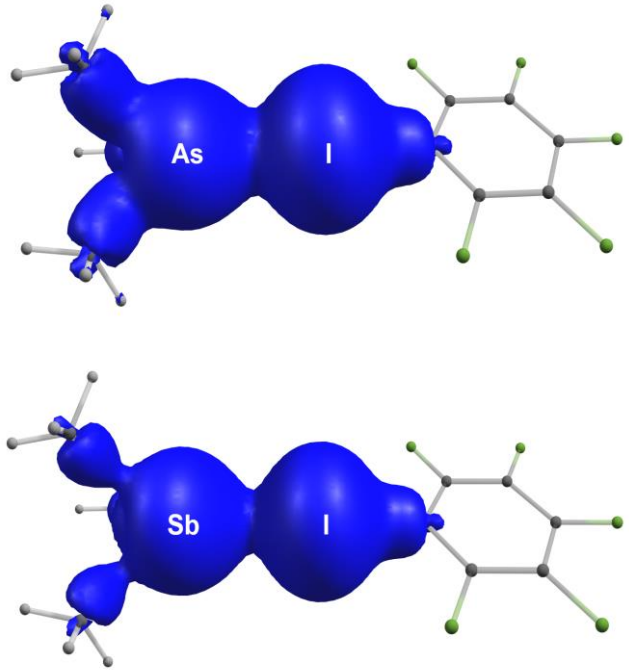

Figure S4. The DID plots of $(CH_3)_3E\cdots IC_6F_5$ at 10^{-5} e Bohr^{-3}. E = As or Sb.

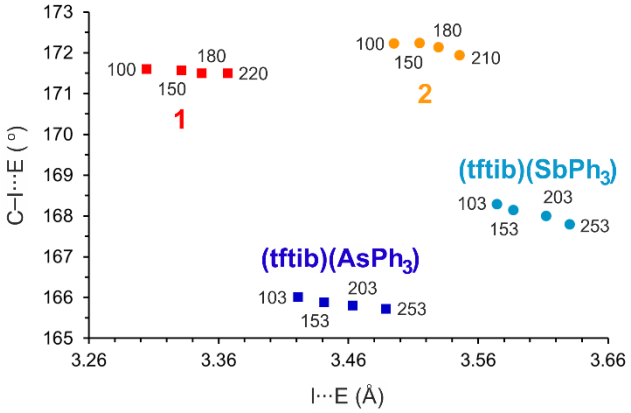

Figure S5. The I···E distances dependence of C–I···E angles for intermolecular interactions C–I···E (E = As or Sb) in **1** ■, **2** ●, as well as cocrystals of 1,3,5-trifluoro-2,4,6-triiodobenzene with triphenylarsine (tftib)($AsPh_3$) ■, and -stibine (tftib)($SbPh_3$) ●, at low temperatures between 100 and 253 K (temperature in K is marked close to the points).[21]

References

1 R. Blom, A. Haaland and R. Seip, *Acta Chem. Scand. A*, 1983, **37**, 595–599.

2 (*a*) A. Bondi, *J. Phys. Chem.*, 1964, **68**, 441–451; (*b*) S. S. Batsanov, *Inorg. Mater.*, 2001, **37**, 871–885; (*c*) S.-Z. Hu, Z.-H. Zhou, Z.-X. Xie and B. E. Robertson, *Z. Kristallogr.*, 2014, **229**, 517–523.

3 (*a*) H. J. Frohn, S. Görg, G. Henkel and M. Läge, *Z. Anorg. Allg. Chem.*, 1995, **621**, 1251−1256; (*b*) M. Bujak, H.-G. Stammler and N. W. Mitzel, *Cryst. Growth Des.*, 2020, **20**, 3217−3223.

4 M. J. Frisch, G. W. Trucks, H. B. Schlegel, G. E. Scuseria, M. A. Robb, J. R. Cheeseman, G. Scalmani, V. Barone, B. Mennucci, G. A. Petersson, H. Nakatsuji, M. Caricato, X. Li, H. P. Hratchian, A. F. Izmaylov, J. Bloino, G. Zheng, J. L. Sonnenberg, M. Hada, M. Ehara, K. Toyota, R. Fukuda, J. Hasegawa, M. Ishida, T. Nakajima, Y. Honda, O. Kitao, H. Nakai, T. Vreven, J. A. Montgomery, Jr., J. E. Peralta, F. Ogliaro, M. Bearpark, J. J. Heyd, E. Brothers, K. N. Kudin, V. N. Staroverov, R. Kobayashi, J. Normand, K. Raghavachari, A. Rendell, J. C. Burant, S. S. Iyengar, J. Tomasi, M. Cossi, N. Rega, J. M. Millam, M. Klene, J. E. Knox, J. B. Cross, V. Bakken, C. Adamo, J. Jaramillo, R. Gomperts, R. E. Stratmann, O. Yazyev, A. J. Austin, R. Cammi, C. Pomelli, J. W. Ochterski, R. L. Martin, K. Morokuma, V. G. Zakrzewski, G. A. Voth, P. Salvador, J. J. Dannenberg, S. Dapprich, A. D. Daniels, O. Farkas, J. B. Foresman, J. V. Ortiz, J. Cioslowski and D. J. Fox, *Gaussian 09*, Revision A.02, Gaussian, Inc., Wallingford CT (USA), 2009.

5 R. Dennington, T. Keith and J. Millam, *GaussView 5.0*, Semichem Inc., Shawnee Mission, KS (USA), 2009.

6 (*a*) A. D. Becke, *Phys. Rev. A*, 1988, **38**, 3098–3100; (*b*) C. Lee, W. Yang and R. G. Parr, *Phys. Rev. B*, 1988, **37**, 785–789.

7 K. Raghavachari, G. W. Trucks, J. A. Pople and M. Head-Gordon, *Chem. Phys. Lett.*, 1989, **157**, 479–483.

8 K. A. Peterson and T. H. Dunning, *J. Chem. Phys.*, 2002, **117**, 10548–10560.

9 K. A. Peterson and K. E. Yousaf, *J. Chem. Phys.*, 2010, **133**, 174116.

10 D. A. Matthews, L. Cheng, M. E. Harding, F. Lipparini, S. Stopkowicz, T.-C. Jagau, P. G. Szalay, J. Gauss and J. F. Stanton, *J. Chem. Phys.*, 2020, **152**, 214108.

11 C. Adamo and V. Barone, *J. Chem. Phys.*, 1999, **110**, 6158–6170.

12 S. Grimme, S. Ehrlich and L. Goerigk, *J. Comput. Chem.*, 2011, **32**, 1456–1465.

13 M. J. Frisch, M. Head-Gordon and J. A. Pople, *Chem. Phys. Lett.*, 1990, **166**, 275–280.

14 M. Gerenkamp and S. Grimme, *Chem. Phys. Lett.*, 2004, **392**, 229–235.

15 M. J. Frisch, G. W. Trucks, H. B. Schlegel, G. E. Scuseria, M. A. Robb, J. R. Cheeseman, G. Scalmani, V. Barone, G. A. Petersson, H. Nakatsuji, X. Li, M. Caricato, A. V. Marenich, J. Bloino, B. G. Janesko, R. Gomperts, B. Mennucci, H. P. Hratchian, J. V. Ortiz, A. F. Izmaylov, J. L. Sonnenberg, D. Williams-Young, F. Ding, F. Lipparini, F. Egidi, J. Goings, B. Peng, A. Petrone, T. Henderson, D. Ranasinghe, V. G. Zakrzewski, J. Gao, N. Rega, G. Zheng, W. Liang, M. Hada, M. Ehara, K. Toyota, R. Fukuda, J. Hasegawa, M. Ishida, T. Nakajima, Y. Honda, O. Kitao, H. Nakai, T. Vreven, K. Throssell, J. A. Montgomery Jr., J. E. Peralta, F. Ogliaro, M. J. Bearpark, J. J. Heyd, E. N. Brothers, K. N. Kudin, V. N. Staroverov, T. A. Keith, R. Kobayashi, J. Normand, K. Raghavachari, A. P. Rendell, J. C. Burant, S. S. Iyengar, J. Tomasi, M. Cossi, J. M. Millam, M. Klene, C. Adamo, R. Cammi, J. W. Ochterski, R. L. Martin, K. Morokuma, O. Farkas, J. B. Foresman and D. J. Fox, *Gaussian 16*, Revision B.01, Gaussian Inc. Wallingford CT (USA), 2016.

16 C. Riplinger, P. Pinski, U. Becker, E. F. Valeev and F. Neese, *J. Chem. Phys.*, 2016, **144**, 024109.

17 F. Neese, *Wiley Interdiscip. Rev. Comput. Mol. Sci.*, 2012, **2**, 73–78.

18 W. B. Schneider, G. Bistoni, M. Sparta, M. Saitow, C. Riplinger, A. A. Auer and F. Neese, *J. Chem. Theory Comput.*, 2016, **12**, 4778–4792.

19 A. Altun, F. Neese and G. Bistoni, *J. Chem. Theory Comput.*, 2019, **15**, 215–228.

20 A. Wuttke and R. A. Mata, *J. Comput. Chem.*, 2017, **38**, 15–23.

21 K. Lisac, F. Topić, M. Arhangelskis, S. Cepić, P. A. Julien, C. W. Nickels, A. J. Morris, T. Friščić and D. Cinčić, *Nat. Commun.*, 2019, **10**, 61.